hydrology

MDPI

Article

Sustainable Water Management in a Complex Watershed: A Case Study in Tulancingo Valley, Mexico

Georgina Itandehui Ávila-Castañeda [1], Elena María Otazo-Sánchez [1,2,*], Silvia Chamizo-Checa [3,*], Gabriela Marisol Vázquez-Cuevas [4] and Alma Delia Román-Gutiérrez [1,*]

[1] Academic Area of Chemistry, Institute of Basic Sciences and Engineering, Hidalgo State Autonomous University, Carretera Pachuca-Tulancingo Km 4.5, Mineral de la Reforma 42184, Hidalgo, Mexico; av483030@uaeh.edu.mx
[2] Council of Science, Technology, and Innovation of Hidalgo, Science Building, Ex Hacienda la Concepción, San Agustín Tlaxiaca 42162, Hidalgo, Mexico
[3] School of Agrobiology, Autonomous University of Tlaxcala, Autopista Tlaxcala-San Martin Texmelucan Km 10.5, Ixtacuixtla de Mariano Matamoros 90120, Tlaxcala, Mexico
[4] Science and Technology Park, Hidalgo State Autonomous University, San Agustín Tlaxiaca 42162, Hidalgo, Mexico; gabriela_vazquez@uaeh.edu.mx
* Correspondence: elenamariaotazo@gmail.com (E.M.O.-S.); silchamiz@gmail.com (S.C.-C.); aroman@uaeh.edu.mx (A.D.R.-G.)

Abstract

This research analyzes water availability in the Tulancingo Valley (Hidalgo State, Mexico), a representative region with notable industrial and agricultural activities, over the period from 2013 to 2050. A conceptual model was developed and calculated with the Water Evaluation and Planning System (WEAP) simulation platform, calibrated with 2014 data, to estimate future water demand under mitigation scenarios that incorporate inertial population and industrial growth, as well as projected climate change trends. The simulation identifies the key actions that support sustainable water-resource management. Results show that agricultural groundwater demand is the dominant pressure on the aquifer, which is projected to become overexploited by 2050 (-185.65 hm^3). The most effective mitigation strategies involve increasing the use of available surface water in both industrial and agricultural sectors; under these measures, the aquifer could recover and reach an annual availability of 231.7 hm^3, ensuring long-term water sustainability of the valley. The modeling approach applied here offers a useful framework for similar assessments in other complex areas.

Keywords: water demand management; climate change; hydrological modeling; water availability scenarios

Check for updates

Academic Editors: Hao Chen, Linjing Qiu and Wenbin Ding

Received: 23 January 2026
Revised: 23 February 2026
Accepted: 25 February 2026
Published: 28 February 2026

Copyright: © 2026 by the authors. Licensee MDPI, Basel, Switzerland. This article is an open access article distributed under the terms and conditions of the Creative Commons Attribution (CC BY) license.

1. Introduction

Water constitutes a fundamental resource for sustaining life, with direct consumption and extensive utilization across agriculture, industry, and energy production, underscoring its critical biological and socioeconomic significance [1]. Approximately 30% of the world's accessible freshwater is stored as groundwater within aquifers, which are unevenly distributed across diverse geographic regions [2]. Furthermore, the fragmentation of global water resources poses substantial challenges to their availability and impedes the implementation of sustainable, integrated water management strategies [3].

Currently, global water demand is approximately 4.6 trillion cubic meters per year, and nearly 2.5 billion individuals worldwide rely directly on groundwater extraction to support

both basic survival and economic development [4]. Moreover, rapid global population growth is intensifying pressure on water resources, further widening the gap between projected demand and available supply. By 2050, global water demand is expected to increase by approximately 55% [5], and about 70% of the world's accessible freshwater is currently allocated to agricultural and livestock production, a situation exacerbated by growing food demand [3].

Water scarcity has emerged as an increasingly urgent global concern, further intensified by climate change, underscoring the need for effective water governance frameworks that address both water demand and resource availability [6]. In this context, numerous studies have used the Water Evaluation and Planning System (WEAP) for hydrological modeling to develop demand-mitigation scenarios that optimize integrated water-resource management and enhance water security. The effectiveness of WEAP for regional and basin-scale water-management scenarios was reviewed by Guo in 2025, who highlighted its widespread use for projecting future water demand, assessing socioeconomic impacts, and designing strategies to address supply–demand imbalances—such as conservation measures, infrastructure improvements, and policy interventions—to ensure a sustainable water supply [7].

Several case studies have adopted this approach for hydrological modeling, including water balance assessments of Lake Titicaca [8] and numerous river basins such as the Central Asia Mountains in Georgia for rivers above 3000 m [9], the Upper Indus River Basin [10], and the complex transboundary Tigris–Euphrates Basin [11]. Many studies evaluate the sustainability of water supply and demand to assess water scarcity and reductions in supply, as seen in Niger [12]. In contrast, others focus on agricultural irrigation and propose targeted management strategies in Ghana [13] and Pakistan [14].

The impact of climate change on future water resources has also been widely examined due to alterations in hydrological cycles, unpredictable precipitation patterns, and the resulting environmental, social, and economic disruptions. Examples include studies in Pakistan [14], Indonesia [15], and Bolivia's Lake Moa Basin [16], which assess irrigation demands under different water availability conditions and propose mitigation strategies to promote sustainable agricultural water management. A recent proposal integrates machine learning techniques with the WEAP model to enhance mitigation strategies for surface water distribution under climate variability, using General Circulation Model projections and satellite data to improve water-resource management [17].

The water–energy–food nexus has likewise become a prominent area of research. Notable examples include studies in the Beijing–Tianjin–Hebei region [18] and methodological applications of the WEAP–LEAP platforms—where LEAP (Low Emissions Analysis Platform) addresses energy demand and associated emissions—in Pakistan [19].

Those reports support the formulation of strategic programs by governments, organizations, and private entities by simulating future scenarios, anticipating hydrological impairment under diverse climatic conditions, thereby reinforcing global water security, encouraging investment in innovative technologies, and enhancing aquifer recharge and recovery processes [1].

To address these water challenges, this study aims to assess water availability in the Tulancingo Valley under various mitigation scenarios for water demand across multiple sectors by 2050 using the WEAP platform, to identify the most effective measures that support sustainable water-resource management and prevent aquifer overexploitation.

The Tulancingo Valley represents an appropriate and complex case study due to its diverse economic activities and its similarities to other regions in Mexico and across developing countries. To date, only one published study has evaluated the aquifer's vulnerability to potential contamination [20]. Consequently, this work constitutes the first

comprehensive assessment of the aquifer's availability, integrating hydrological modeling with long-term management strategies. Unlike the previous study, which focused exclusively on contamination risks, this research addresses resource availability and sustainable management practices.

2. Materials and Methods

2.1. Study Area

The Tulancingo Valley is in the central-eastern region of Mexico, within the southeastern portion of the state of Hidalgo, between latitudes 19°56′ and 20°17′ N and longitudes 98°12′ and 98°32′ W, covering an area of approximately 1183 km^2 [21]. The valley comprises the municipalities of Acatlán, Acaxochitlán, Cuautepec de Hinojosa, Metepec, Singuilucan, Santiago Tulantepec de Lugo Guerrero, Tulancingo de Bravo, and Chignahuapan. Topographic elevations range from 1640 to 3180 m above sea level. See Figure 1.

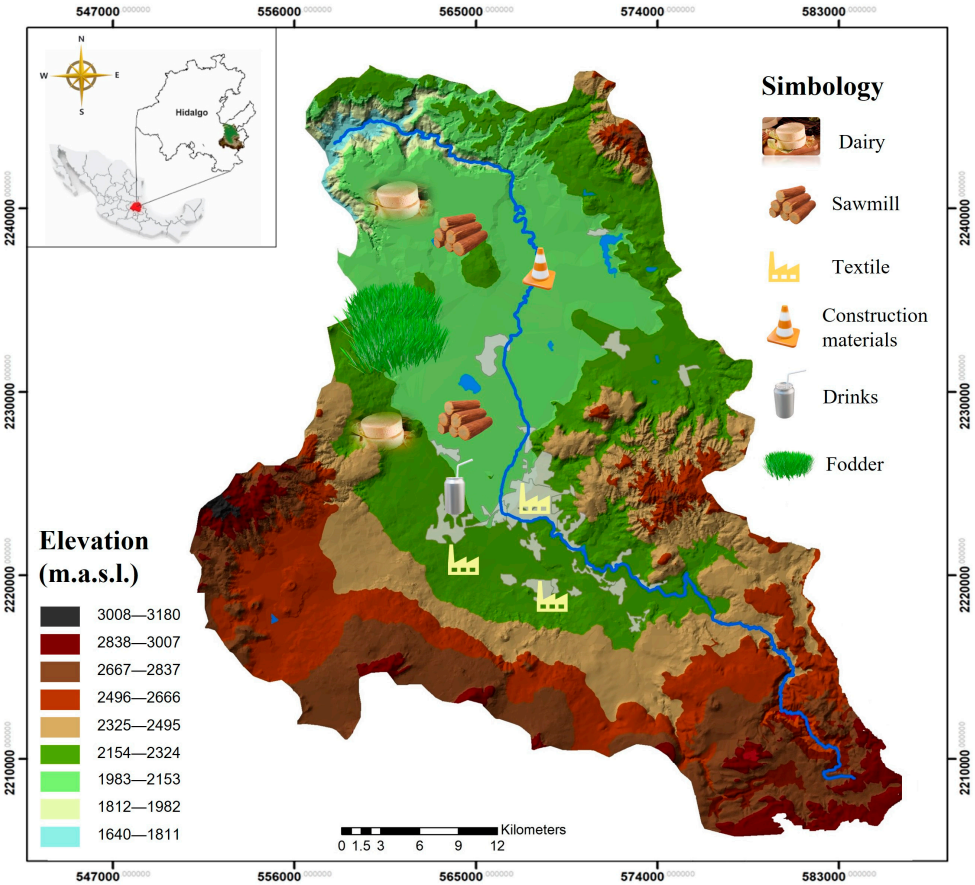

Figure 1. Tulancingo Valley, Hidalgo State, Mexico. Source: Author's elaboration based on public data [21,22]. The blue line and the blue spots represent the Grande Tulancingo River and small lagoons. Note: m.a.s.l means meters above sea level.

The total population of the valley is 242,014 inhabitants [22], of whom 71% are concentrated in the municipalities of Tulancingo de Bravo and Cuautepec de Hinojosa. The main economic activity and land use in the area focus on agricultural and livestock production.

2.1.1. Climatological and Soil Parameters

The prevailing climate in the Tulancingo Valley is semi-arid steppe with summer rainfall. The predominant soil types include kastanozems, vertisols, luvisols, and umbrisols [23].

Monthly accumulated precipitation and temperature data were obtained from the historical series for the period 1998 to 2017, available from the Mexican Meteorological Services public data [24], as detailed in Figure S1 of the Supplementary Material. Data from 15 representative weather stations were compiled and systematized for the model. These stations were selected using the Thiessen polygon interpolation method [25]. The months of June, July, August, and September have the highest precipitation. The lowest annual average rainfall (400–500 mm) occurs in the central region, in the municipalities of Santiago Tulantepec and a small portion of Tulancingo de Bravo. In contrast, the rest of the municipalities receive between 500 and 800 mm annually [24].

The average annual temperature in the area ranges from 12 °C to 18 °C (Figure S1), with a predominant range of 14–16 °C in the municipalities of Acatlán, Tulancingo de Bravo, and Santiago Tulantepec and 12–14 °C in Cuautepec de Hinojosa, Singuilucan, and Metepec [24].

2.1.2. Hydrological Parameters

The Tulancingo Valley is located within Hydrological Region 26 Alto Pánuco. Figure 2 shows the surface and groundwater hydrology of the valley; notice that the 824 ha Irrigation District 028 serves 484 users. The annual volume of surface water allocated for irrigation is 13,366,050 m^3 [20,26,27]. Additionally, the reported industrial and municipal wastewater allocations, along with surface and groundwater volumes, were used to calculate parameters for each sector, and 284 wells were identified within the study area [26].

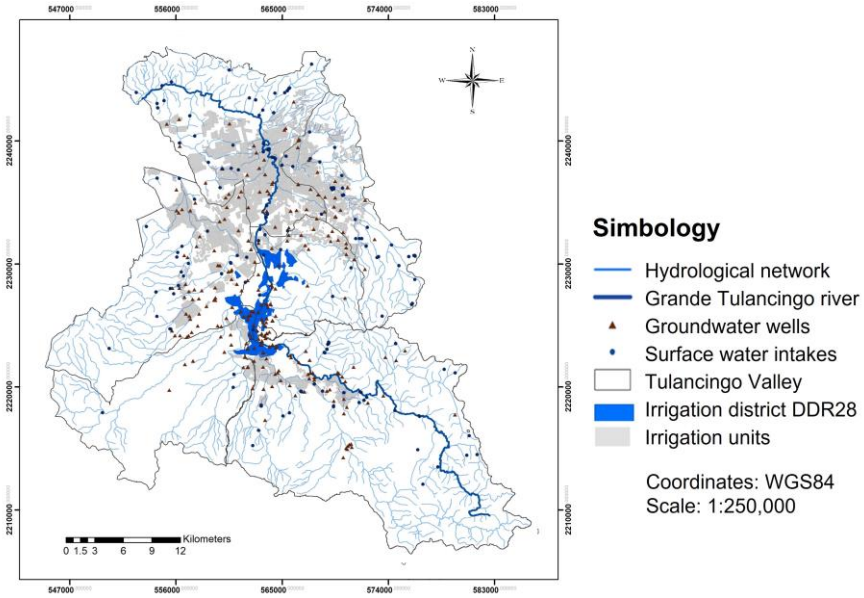

Figure 2. Hydrological network of the Tulancingo Valley. Source: Author's elaboration based on public data [22,26].

The 1317 Valle de Tulancingo aquifer [28] is semiconfined and serves as the primary source of potable water for the valley. The total concession volume allocation activities allocate 78.5% to agricultural and livestock, 18.8% to urban public, 1.85% to domestic, and 2.0% to industrial [29].

The aquifer system comprises two distinct horizons. The deeper aquifer extends beneath the entire valley and serves as the region's primary groundwater source. Its main recharge zones are in the surrounding mountainous areas to the south, west, and east of the valley. Natural outflows occur in the northern sector, where groundwater emerges,

and surface water flows toward the Barranca de Meztitlán ravine. The shallow aquifer is situated above a compact, impermeable basaltic layer that limits vertical percolation [30].

2.2. Conceptual Model Boundaries

To ensure clarity and analytical rigor, the boundaries of the conceptual model are defined by spatial extent, temporal scope, and thematic focus. The model serves as a synthesis of the data and assumptions used to develop the subsequent mathematical model in WEAP.

- The base year was set as 2013, as it represents a normal year according to the standardized precipitation index (Figure S2 in Supplementary Material). The hydrometric station 26,807 is the only one in the whole valley, and its historical data unfortunately ended in 2014, with incomplete data (1982–2014). The 2013 information is the best available for calibration of the mathematical model.
- Tulancingo Valley is considered a watershed for the study. Based on elevation maps, it holds six sub-basins for study: Cuautepec, Acatlán, Barranca, Tulantepec, Metepec, and Napateco (see Figure 3). Each sub-basin has a principal tributary converging into the Grande Tulancingo River.

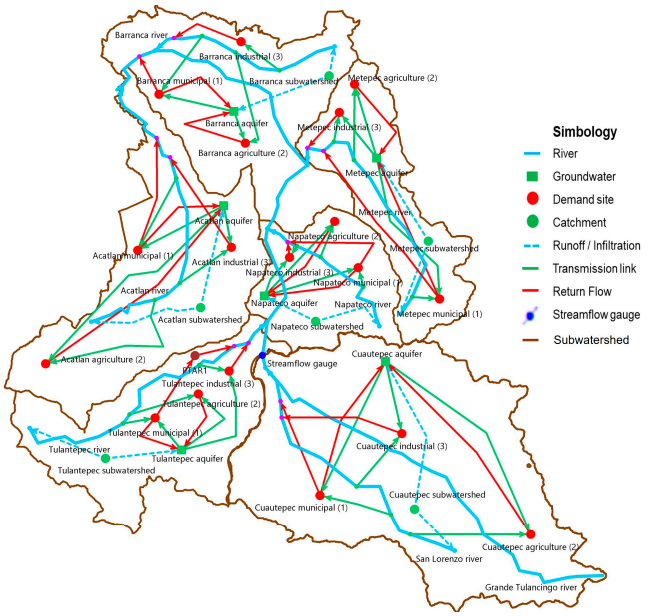

Figure 3. Schematic model of the study area developed in WEAP with delimited sub-basins. Sub-Basin Main Characteristics in 2013.

- The Grande Tulancingo River is the main tributary of the valley, originating from the mountainous region of Chignahuapan (state of Puebla) and flowing northward (see Figure 2) toward the Barranca de Meztitlán, carrying rainfall, municipal, and industrial wastewater. It is the main supplier of surface water.
- There is no external inflow, because the Grande-Tulancingo and San Lorenzo rivers originate internally, from the runoffs of the Chignahuapan mountains, Puebla, at the southern border of the Cuautepec sub-basin.
- Approximately 500 geological faults (sinkholes) occur in the southern part of the valley, increasing infiltration rates, mainly in the Cuautepec sub-basin [31].
- Surface water inputs include the following: (1) flows from the Chignahuapan mountains via the Grande Tulancingo and San Lorenzo rivers at the southern border of the valley, (2) rainfall runoff, and (3) municipal (domestic and public services) and industrial wastewater.

- Surface water outputs include the following: (1) evapotranspiration and (2) outflow toward the ravine "Barranca del Meztitlán" in the northern part of the valley, and (3) demands include the following: (a) agriculture and livestock, (b) urban (public services), and (c) industrial.
- The groundwater supplier of the studied area is the Tulancingo Valley aquifer, which has two horizons: (1) shallow, confined (20–40 m deep), and (2) deep (up to 300 m), and the latter is semiconfined [30]. Groundwater availability is 103 hm^3 [32].
- Groundwater inputs are as follows: (1) aquifer recharge through rainfall infiltration and sinkholes, and (2) irrigation return flows (irrigation of public gardens was discarded). There is no underground water transfer from other aquifers.
- Groundwater outputs are as follows: (1) groundwater outflows (4.4 hm^3) driven to the fractured strata of Meztitlán ravine [30] and (2) demand (pumping) from (a) agriculture and livestock, (b) urban (domestic, public services, and commerce), and (c) industrial (notably textiles, soft drinks and beverages, dairy products, construction materials, and sawmills).
- Evapotranspiration will be estimated using the Penman–Monteith method.
- Climate projection uncertainty is not quantified. The SSP3-RCP7.0 forecast was considered without exploring another climate scenario.
- Groundwater consumed by the soft drink industry represents a minor export, and the model, therefore, treats its production volume as negligible.
- Further mathematical model considerations are as follows: (1) exclusion of induced pasture due to rainfed agriculture, and (2) the Cuautepec sub-basin will be used for calibration because the unique hydrometric station (26,807 Tulancingo) is located downstream of the Grande Tulancingo River after the San Lorenzo River input and is assumed valid for the entire valley.

Figure 3 shows the natural boundaries of the sub-basins and their principal rivers, as well as the schematic scheme used in the mathematical model. Table 1 summarizes relevant data for the sub-basins in the base year 2013.

Table 1. Area, population, primary industries, and land use in the Tulancingo Valley in the base year 2013.

Sub-Basin	Area (km^2)	Pop (Inhab)	Industrial Sector (Number of Industries) *				Land Use Percentage (%)						
			Tex	Saw	FI	CM	TA	IA	UA	F	P	WB	SC
Napateco	98	17,634	60	4	29	41	25.5	35.0	8.5	15.9	11.9	0.02	3.1
Metepec	116	12,162	7	1	2	17	59.4	14.3	1.2	20.7	2.2	1.6	0.7
Tulantepec	167	92,881	47	0	24	20	60.1	6.0	3.6	29.6	0.4	0.1	0.0
Barranca	198	10,608	0	1	0	4	51.7	17.0	0.08	23.0	4.3	0.15	3.7
Acatlán	219	35,455	4	0	77	10	38.7	27.5	1.4	27.4	4.4	0.5	0.07
Cuautepec	385	73,274	139	0	45	67	55.6	5.6	3.4	26.7	7.5	0.05	1.0
Valley	1183	242,014	257	6	177	209	50.3	14.9	2.7	25.1	5.2	0.3	1.3

Note: the predominant municipality named some sub-basins, but this does not align with the reported municipal political division. Pop: population * [22], Tex: textile industry, Saw: sawmill, FI: food industry, CM: construction materials, TA: rainfed agriculture, IA: irrigated agriculture, UA: urban areas, F: forest, P: pastureland, WB: water bodies, SC: scrub crasicaule.

- Cuautepec sub-basin: Located in the valley's southeastern part, this sub-region marks the initial segment where the principal river enters the valley. It is the largest in territorial extent, with 56% allocated to rainfed and surface water agriculture and 6% to irrigated agriculture and livestock activities. It hosts the largest textile and distilled beverage industries and ranks second in population, accounting for 30% of the valley's total.

- Tulantepec sub-basin: Located in the southwestern zone of the valley, it accounts for the region's highest population concentration, representing approximately 38% of the total. This sub-basin is characterized by extensive rainfed barley cultivation, 47 textile industries, and a slaughterhouse, all of which exert additional pressure on groundwater resources.
- Metepec sub-basin: Located in the east of the valley, it produces maize grain and red tomatoes under irrigated agriculture, hosts a sawmill and four small-scale stone extraction industries. It contains only 5% of the valley's population.
- Napateco sub-basin: Located in the center of the valley, it presents the smallest surface, with urban zones accounting for 7% of the total population and a natural park. It exhibits the highest level of alfalfa production in the region, supported by the groundwater gravity-irrigated Tulancingo Irrigation District, 75% of which is located within this sub-basin.
- Acatlán sub-basin: Located in the western part of the basin, it is the second largest territorial extent with notable high agricultural and livestock activity, which relies on groundwater. It excels in forage crop production under irrigation (135,711 t) and livestock farming, producing 1062 t of meat and 19.14 million liters of milk [33], and it hosts 61% of dairy-producing small businesses, generating 29,275 L/day of untreated whey discharges into drains, rivers, or soil [34]. This sub-basin accounts for 15% of the valley's population.
- Barranca sub-basin: Located in the basin's northernmost part, this region marks the final segment where the principal river discharges into the ravine Barranca de Meztitlán. It leads to regional production of red tomatoes under greenhouse conditions and ranks second in grain maize output. The area also hosts stone extraction and the construction materials industry. It has the lowest population share in the basin, accounting for only 4% of the total population.

2.3. Mathematical Model

Surface and groundwater volumes for both the baseline year and projected scenarios were calculated using the Water Evaluation and Planning System (WEAP v2025.0.11.0) software [35]. The results are used to determine the aquifer's water balance and the valley water metabolism and to characterize the hydrological cycle within the study area.

The WEAP schematic model (Figure 3) uses a vector layer created in ArcGIS that includes the representative sub-basins of the study area, the principal interactions between sectorial demands sites and the primary water sources (Grande Tulancingo River and aquifer), as well as the hydrological units, infiltration, return flows, and runoff processes.

2.3.1. Sub-Basins Delimitation

Sub-basin delineation. The topographic map of the state of Hidalgo [36] facilitated delineation of sub-basin boundaries using the "Hydrology" tool in the "Spatial Analyst Tools" suite.

Simulation of the valley's hydrological cycle. The "rainfall runoff" module provides greater data availability for the required parameters [37] to calculate the hydrological cycle for each sub-basin and the whole valley by summing the partial results.

Interpolation of precipitation using kriging. We used public climatic data from the National Meteorological Service (SMN) online platform [24] to calculate average values based on records from 15 meteorological stations within the study area. Figure 4A shows a raster map of monthly and annual rainfall interpolated using kriging in ArcGIS 10.5, for each sub-basin.

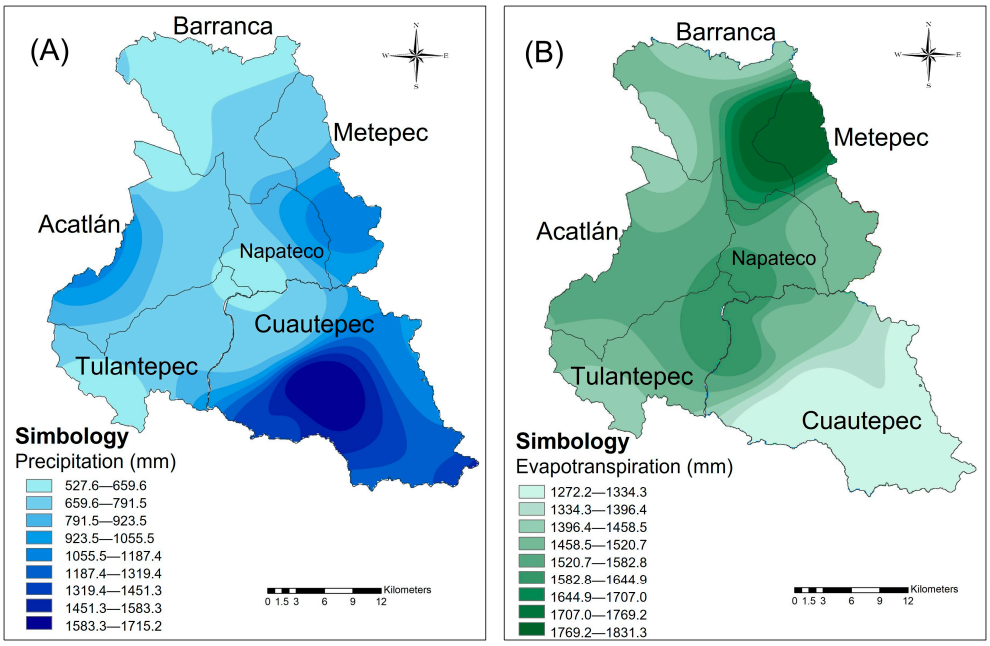

Figure 4. Kriging interpolation of (**A**) precipitation and (**B**) evapotranspiration.

Evapotranspiration calculation (ETo). The standardized Penman–Monteith method (Equation (S1)) is accepted and recommended by the World Meteorological Organization and adopted by the FAO to calculate monthly ETo for the base year 2013 [38]. Figure 4B shows the resulting interpolated raster map.

Determination of runoff (*Cr*) and infiltration (*Ci*) coefficients. For the runoff coefficient (*Cr*), we applied Equation (1) following the methodology reported by [39], which considers slope, soil texture, land use, and a 10-year return period for each sub-basin. Equation (2) is the current method for calculating the infiltration coefficient (*Ci*) by subtracting the runoff coefficient from 1. Table 2 displays the results for each sub-basin.

$$Cr = LU + S + T \quad (1)$$

where Ce: runoff coefficient, *LU*: land use, *S*: slope, and *T*: texture

$$Ci = 1 - Cr \quad (2)$$

Table 2. Runoff and infiltration coefficients obtained for each sub-basin (%).

Sub Watershed	Area (km^2)	Cr	Ci
Napateco	98	43.76	56.24
Metepec	116	43.11	56.89
Tulantepec	167	42.07	57.93
Barranca	198	41.02	58.98
Acatlán	219	40.41	59.59
Cuautepec	385	38.00	62.00
Tulancingo Valley	1183		

Note: the predominant municipality named some sub-basins, but they do not match the municipal political division. Cr: runoff coefficient, Ci: infiltration coefficient.

2.3.2. Calculation of Crop Coefficient (Kc) and Water Demand

Crop coefficient (Kc). Table 3 displays the obtained Kc and crop yields, calculated considering the growth periods of each crop (alfalfa, oats, grain maize, forage maize, ryegrass pasture, and tomato), along with the water requirements for each phenological stage.

Table 3. Crop coefficients (Kc) and crop yields of representative crops in the Tulancingo Valley.

Crop	Kc												Yield (t/ha)
	Jan	Feb	Mar	Apr	May	Jun	Jul	Aug	Sep	Oct	Nov	Dec	
Alfalfa	0.95	0.95	0.05	0.05	1.15	1.15	1.15	1.00	1.10	1.00	0.05	0.95	86.80
Oats	0.95	0.95	0.05	0.05	1.31	1.6	1.46	0.95	0.95	0.05	0.00	0.05	1.81
Tomato	0.05	0.05	0.05	0.05	1.01	1.07	1.16	0.95	0.95	0.5	0.05	0.05	200.45
Forage corn	0.95	0.05	0.05	0.05	1.08	0.94	1.5	0.95	1.04	0.95	0.00	0.05	40.06
Grain corn	0.95	0.95	0.05	0.05	1.08	0.94	1.5	0.95	1.04	0.92	0.00	0.00	3.00
Grasses	0.10	0.70	0.05	0.05	1.11	0.95	1.11	0.95	1.50	0.80	0.80	0.70	86.20
Green tomato	0.95	0.95	0.05	0.05	1.10	0.30	1.10	0.95	1.10	0.50	0.00	0.05	26.49

Water demands calculation. Surface and groundwater volumes were estimated using official data from the Public Water Rights Registry (REPDA) of [26], a publicly accessible online database. As the records are organized by municipality and sector, each entry was georeferenced to determine its corresponding sub-basin. Industrial water demand was calculated by identifying relevant industry types listed in the National Statistical Directory of Economic Units (DENUE) [22] for the baseline year (Table 1) and applying the specific water allocation for each industry type's production processes. The dairy industry comprises 75 small businesses in the Acatlán and Tulantepec sub-basins, whose water demand was estimated using the methodology reported in [40], based on the relation between milk production volumes and the water required for processing.

2.3.3. Calibration and Validation

Calibration. The unique hydrometric station is located downstream of the confluence of two rivers, in the Cuautepec sub-basin, and its flow gauge data were valuable for model calibration, as evidenced by the linear correlation between the monthly surface water volumes calculated and reported by hydrometric station 26,807 on the Grande Tulancingo River, based on 2013 flow data. We excluded the May value because the hydrometric station volume was unreliable for that month. See Figure 5 in Section 3.1.

Validation. The Mean Absolute Percentage Error (MAPE) was calculated using Equation (1) to assess the model's accuracy [41].

$$MAPE = \frac{1}{n}\sum_{i=0}^{n}\frac{|A_t - P_t|}{A_t}\,100 \quad (3)$$

where n is the number of calculated volumes, At is the actual volume, and Pt is the predicted one in the time interval t (month). See results in Section 3.1.

2.3.4. Sensitivity Analysis

The sensitivity analysis was conducted following the methodology in [35] by modifying the crop coefficient (Kc) values for grain maize across the entire valley, using the minimum and maximum values reported in [42], as shown in Table 4. This crop was selected because its production occupies more than 60% of the total land area devoted to irrigated agriculture.

Table 4. Kc values for grain maize used in the sensitivity analysis.

Kc	Jan	Feb	Mar	Apr	May	Jun	Jul	Aug	Sep	Oct	Nov	Dec
Used	0.95	0.95	0.05	0.05	1.08	0.94	1.50	0.95	1.04	0.92	0.001	0.001
Maximun	1.00	1.00	0.30	0.40	1.50	1.50	1.50	1.50	1.50	1.20	0.30	0.30
Minimun	0.30	0.30	0.05	0.05	0.40	0.90	0.70	0.70	0.70	0.60	0.001	0.001

2.3.5. Water Metabolism in the Valley

The fundamental components of the water outflows and inflows, as well as the sectoral demands and interchanges, were represented in Sankey diagrams, which were helpful for visual representation. The differences between initial inflows and final outflows are attributed to internal changes in soil moisture and in aquifer storage.

2.3.6. Water Balance Calculation of the Aquifer

The water balance was calculated by Equation (4), where the left and right sides represent total inputs = total outputs + storage change. The volumes are expressed in hm^3/year.

$$R + I = Qgr + D + \Delta S \quad (4)$$

where R is the average annual total recharge, I is infiltration, artificial, or return flows, Qg is the volume of groundwater extraction (pumping), D is the compromised natural discharge and springs, and ΔS is the change in groundwater storage and soil.

2.3.7. Water Stress Index

Hydric stress was assessed using the Falkenmark Index (FI), widely recognized for evaluating water scarcity in relation to population dynamics [43]. This index requires data on the number of inhabitants in each region and the volume of water from aquifers, rivers, and lakes available for domestic, agricultural, and industrial use. See Equation (5). A value below 1700 m^3 per capita per year indicates hydric stress or water scarcity (see the thresholds in Table S1).

$$IF = \frac{Total\ renewable\ water\ resources}{Population} \quad (5)$$

2.4. Transient Scenarios

2.4.1. Inertial Growth Scenario (BAU)

The inertial scenario (usually named "Business as Usual", BAU) considers annual growth or decline rates in population, agricultural areas, urban zones, forest cover, and the industrial sector to estimate increased water demand in each sub-basin over the simulation period 2013–2050, without accounting for other disturbances.

Table S2 in the Supplementary Material presents municipal-level population growth projections based on official data from the State Population Council [44]. ArcGIS 10.5 allowed disaggregation of population percentage increases by sub-basin, as well as the industrial production units listed in the DENUE [21,22]. Agricultural production projections under irrigation included alfalfa, oats, forage maize, grain maize, ryegrass pasture, red tomato, and green tomato [21]. Calculations were based on the percentage growth rates of the production area reported by the Agricultural and Livestock Information Service for 2015, 2020, and 2022 [45], as detailed in Table 5.

Projections of percentage changes in agricultural, urban, and forest areas were based on land-use change series reported by INEGI [46,47]. We designed a predictive model in MiniTab 18.0 for each type of land-use change across the six sub-basins of the valley Tables S3 and S4), which were input into WEAP using the equation editor as hectare percentages via the "Interp" function every 10 years.

This scenario is unrealistic because it does not incorporate regional climate change projections. Therefore, we designed the following scenario as a better reference for comparison with subsequent mitigation-based scenarios.

Table 5. Growth rates of the urban, industrial, and agricultural plus livestock sectors in each sub-basin (%).

Sub-Basin	Urban *	Industrial **	Agricultural and Livestock ***
Napateco	0.46	1.30	0.29
Metepec	0.66	1.53	0.49
Tulantepec	0.17	1.30	0.01
Barranca	0.63	2.0	0.47
Acatlán	0.23	1.53	0.14
Cuautepec	0.33	1.56	0.20

Note: The predominant municipality named some sub-basins, but they do not match the municipal political division. * [43]; ** [21,22]; *** [45].

2.4.2. Climate Change Scenario (CC): The Reference

This scenario incorporates estimated future climate change effects into the previous BAU scenario, including changes in precipitation, mean temperature, and evapotranspiration for each sub-basin. Short-term (2014–2030) and medium-term (2031–2050) projections of precipitation and mean temperature were taken from the SSP3-RCP7.0 scenario for Mexico, reported by the Intergovernmental Panel on Climate Change [47]. Table 6 presents the variations in precipitation, temperature, and evapotranspiration calculated from temperature projections.

Table 6. Projection of climatic parameters' changes for the SSP3-RCP7.0 projection *.

Parameter	2014–2030	2031–2050
Precipitation (%)	0.4	−1.5
Temperature (°C)	0.7	1.4
Evapotranspiration (%) **	0.073	0.146

* IPCC, 2023. ** Calculated from pre-industrial data (standardized Penman–Monteith method).

2.4.3. Demand Mitigation Scenarios (M1–M5)

Based on the Reference scenario (CC), the mitigation ones (M1–M5) include penetration of actions for water demand compensation across three sectors during the simulation period (2013–2050) gradually. Hence, they are considered perturbations of the reference CC scenario.

Agricultural sector

- Irrigation conveyance efficiency (M1): The perturbation is the maintenance improvement of irrigation canals, including gradual lining to reduce infiltration losses [13]. The penetration assumes an annual water-use depletion of −0.2% for the 2014–2025 period (because it has already occurred) and −1.31% for 2026–2050.
- Sprinkler irrigation (M2): The perturbation is the efficiency improvement from substituting gravity irrigation with sprinkler systems, which can achieve up to 85% in water-efficiency savings [48]. Penetration is projected in steps: −0.2% annually in the 2014–2025 period (because it has occurred) and −2.48% for the 2026–2050 period.
- Groundwater use substitution by surface water (M3): The perturbation focuses on surface water irrigation from rivers or waterbodies to mitigate the high groundwater demand. Penetration is projected in steps across five sub-basins due to flow variability, except for the Cuautepec sub-basin, which relies mainly on rainfall and surface-water irrigation. The substitution steps consider the years 2026, 2030, 2040, and 2050. The corresponding substitution percentages varies upon the surface water availability, as follows: Metepec and Tulantepec (2%, 4%, 10%, and 15%), Barranca (2%, 4%, 4%, and 5%), Acatlán (2%, 4%, 5%, and 6%), and Napateco (2% in 2026 and subsequently 4%).

Urban sector

- Physical efficiency (M4): The perturbation is the water demand reduction by repairing leaks in urban potable water distribution systems (urban areas have 50% physical efficiency in 2013). Penetration starts at 2% in 2020, with an annual efficiency increase of 0.3%, reaching 75% by 2050 [40].

Industrial sector

- Treatment plant for wastewater reuse (M5): Perturbation is estimated to save surface water in textile industries by treating wastewater. Ref. [49] reported a potential 50% substitution in the textile industry. Penetration is considered in 2035, when treatment plants may begin with a conservative 30% substitution.

3. Results and Discussion

3.1. Model Calibration and Validation

Before calculating the water parameters for the Tulancingo Valley, we calibrated the model using the linear correlation between WEAP monthly output volumes and the corresponding volume data from hydrometric station 26807 for the Grande Tulancingo River. The Pearson linear correlation coefficient R for surface waters was 0.971, as shown in Figure 5.

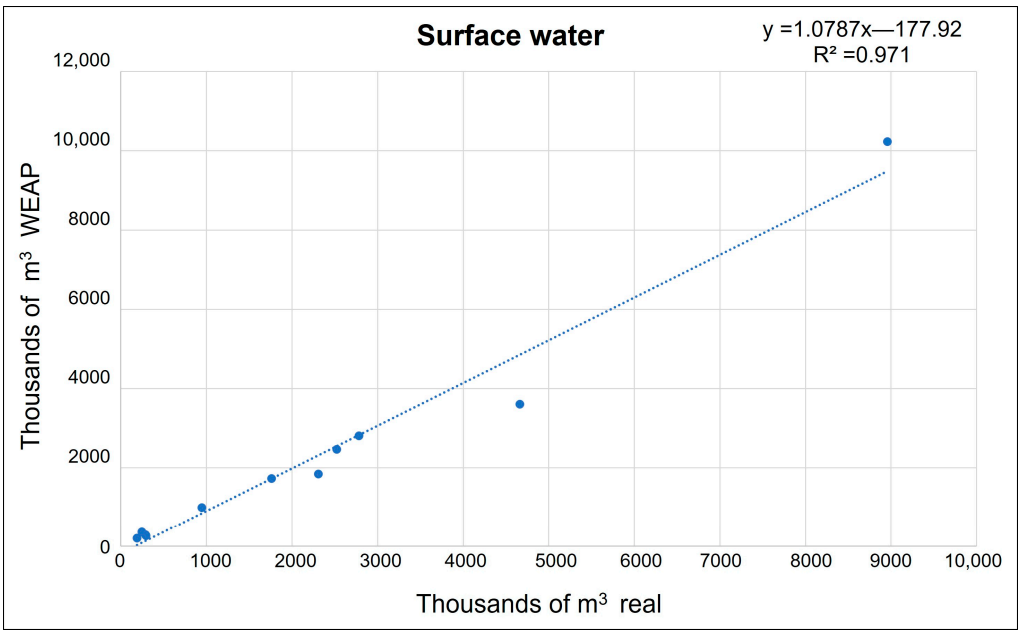

Figure 5. Model validation.

Table 7 presents the differences between the calculated and actual monthly values used to compute the MAPE of 7.92%, providing validation support for the model. Several authors have reported the same procedure with similar accepted results [17,37,40,50].

3.2. Sensitivity Analysis

The sensitivity analysis for maize grain crops Kc is shown in Figure 6A,B for the variations observed in the runoff and infiltration volumes simulated with WEAP.

Figure 6 shows that there are almost no differences between the maximum and minimum values from January to August, and in October and December, with the largest discrepancy occurring in September. In this month, the difference in infiltration reaches 27.75 hm^3, while runoff differs by 19.09 hm^3. In November, the differences are smaller—8.39 hm^3 for infiltration and 5.98 hm^3 for runoff. September is the rainiest month, which

explains both the magnitude of these differences and the higher sensitivity to the maximum and minimum Kc values. In general, the analysis results improve confidence and reliability in the model.

Table 7. Mean Absolute Percentage Error (MAPE).

Month	1000 m^3 Real	1000 m^3 WEAP	MAPE
January	292.55	265.51	9.2
February	190.43	205.39	7.9
March	288.06	283.04	1.7
April	284.86	290.59	2.0
June	1760.40	1732.22	1.6
July	2306.91	1847.88	19.9
August	2523.98	2467.24	2.2
September	8957.78	10,234.88	14.3
October	2781.04	2806.03	0.9
November	4660.93	3604.68	22.7
December	946.94	991.57	4.7
Reliability 92.08%			MAPE: 7.92%

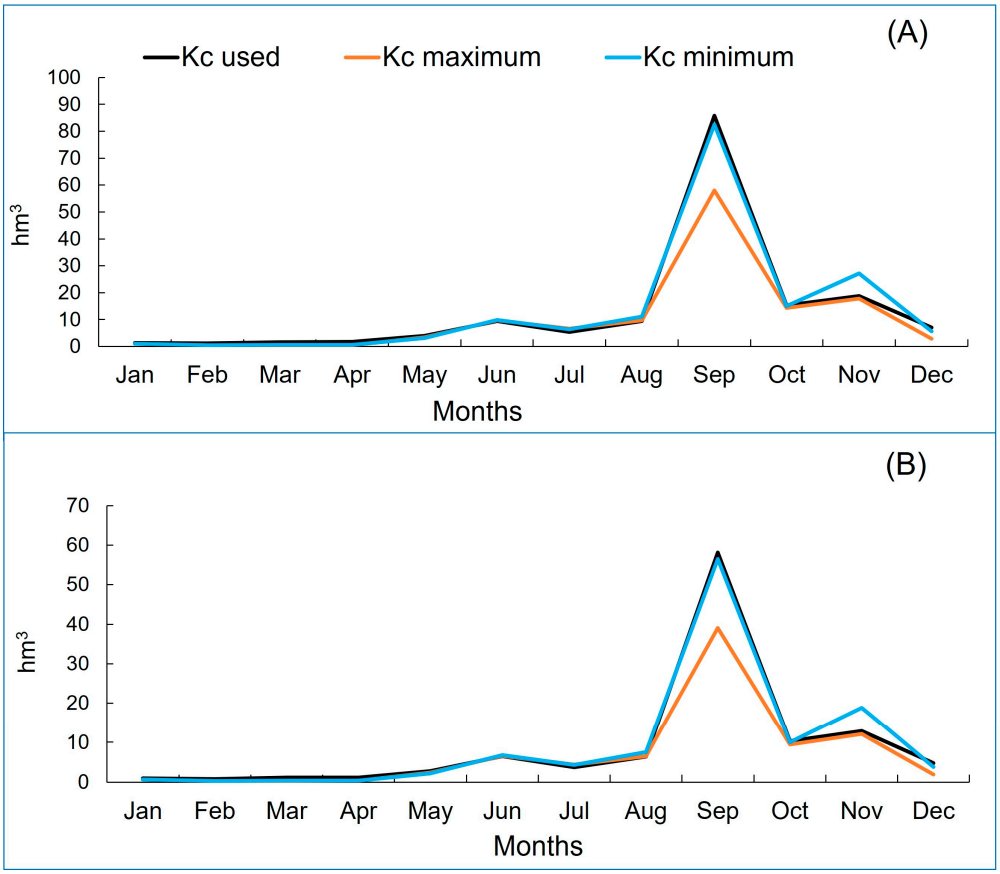

Figure 6. Model sensitivity analysis. (**A**) Infiltration. (**B**) Runoff.

3.3. Surface and Groundwater Demand Analysis in the Baseline Year 2013

Table 8 shows the surface and groundwater demand volumes by sector for the baseline year. Groundwater accounts for 81.8% of total water demand; hence, surface water is underused. Additionally, the agricultural and livestock sector accounts for 91% of the valley's total water demand, a figure considerably higher than the global average (70%) reported by the authors of [3]. This high percentage may be attributed to the valley's low levels of urbanization and industrial activity, particularly in that year.

Table 8. Area (km^2), surface, and groundwater demands * by sector (hm^3) for the sub-basins of the Tulancingo Valley (baseline year 2013).

Sub Basin	Pop (10^3)	Area (km^2)	Surface Water (hm^3)			Groundwater (hm^3)		
	Pop [&]	IA [≠] + Urb	AgLi [§]	Urb	Ind	AgLi [§]	Urb	Ind
Napateco	17.63	34 + 8.3	8.59	0.39	0.36	73.17	1.04	4.05
Metepec	12.16	17 + 1.4	8.63	0.10	0.36	26.80	0.48	0.12
Tulantepec	92.88	10 + 6.1	7.07	0.71	0.44	16.96	3.63	2.24
Barranca	10.60	34 + 0.2	10.1	0.07	0.79	64.66	0.82	NR
Acatlán	35.45	60 + 3.0	12.99	0.17	0.85	115.89	1.88	1.15 [#]
Cuautepec	73.27	22 + 13.2	14.49	0.68	4.80	3.96	3.46	1.20
Tulancingo Valley	242.01	177 + 32.2	61.87	2.12	7.60	301.44	11.31	8.76
			Total demand: 71.59			Total demand: 321.51		

* [26], [&] Pop: population, [≠] IA: irrigated agriculture, Urb: urban, [§] AgLi: irrigated agriculture and livestock sector, Ind: industrial, NR: not reported. [#] Calculated from Annual Operating Certificates of Municipal Companies (Spanish Acronym COA). Note: the predominant municipality named some sub-basins, but they do not match the municipal political division.

3.3.1. Surface Water Demand

The primary surface water demand was identified in the agricultural and livestock sector (86.4%), which accounts for 70.5% of the region, as shown in Table 1.

The Cuautepec sub-basin stands out, representing 20.24% of the total, and has the highest surface water concessions (19.97 hm^3) across all sectors, due to its availability, supported by the presence of two main rivers and water bodies that allow irrigation canals (See Figure 3). Those facts facilitate agricultural and livestock activities based principally on surface water. The Acatlán sub-basin accounts for 18.14% of agricultural surface water use, as runoff from the Huasca Mountains is mainly used for agriculture and cattle raising. Nevertheless, agricultural surface irrigation should be improved.

The urban sector accounts for only 3% of the total available surface water, used mainly for urban services (irrigation of green and sports areas, street cleaning, and infrastructure maintenance) and recreational purposes (artificial lakes and water bodies for leisure). This low percentage is due to the small urban area in the Tulancingo Valley (2.7% of the total area, mainly in the Tulantepec and Cuautepec sub-basins).

In the industrial sector, surface water demand accounted for 10.6% of the total. The Cuautepec sub-basin has the highest value (6.7%), due to the presence of 139 textile industries located [34]. There are many small textile factories, but two are significant and hold concessions totaling 8.1 hm^3 [26] for cooling, manufacturing, and services.

These results highlight the need to implement strategic actions to improve the use of surface water across all three sectors. Primary recommendations should focus on government support for existing and new irrigation canals, emphasizing DDR 028, which covers 824 ha and is mostly irrigated with surface water [27], and on the construction or upgrading of wastewater treatment infrastructure to reduce groundwater extraction in this sector.

The location of surface water and quality sources in the northern downstream sub-basins might not facilitate their use; nevertheless, substituting for agricultural groundwater demand could mitigate this to some extent. Downstream flows carry municipal and industrial wastewater discharges, and the water quality must meet agricultural irrigation standards.

3.3.2. Groundwater Demand

There is a high demand for groundwater from the agriculture and livestock sector, which accounts for 93.8% of total groundwater demand; infiltration from irrigation accounts for only 15%, which is insufficient to meet aquifer demand. The Irrigation District relies mainly on groundwater for agricultural production, with almost exclusive reliance on extraction wells. It is necessary to implement sustainable strategies to reduce groundwater demand and prevent aquifer overexploitation and to consider the available surface water in the area.

The highest groundwater demand (36%) occurs in the Acatlán sub-basin, driven by extensive agricultural and livestock activities. In contrast, Cuautepec exhibits a better hydrological dynamic, with minimal concessions of agricultural groundwater demand (1.2%), since local river use allows predominant reliance on surface water.

In the urban area, the Tulantepec and Cuautepec sub-basins account for 63% of total urban groundwater because they host 69% of the valley's population and, therefore, concentrate the highest number of services and businesses, with concessions registered for urban or service use [26].

The highest industrial groundwater demand occurs in the Napateco sub-basin (46% of total industrial groundwater), due to concessions granted to five textile and beverage industries [26].

The valley consumes poor surface water across the three sectors and a large share of groundwater for agriculture and livestock. As a preliminary conclusion, the sub-basins should be analyzed separately to identify actions to improve surface water management, relieve pressure on the aquifer, and prevent overexploitation.

3.4. Water Balance and Hydric Stress in the Tulancingo Valley for the Baseline Year 2013

The input and output flows were calculated for the baseline scenario. The values for the entire valley are presented in Figure 7, while Figure 8 provides a detailed breakdown for each sub-basin.

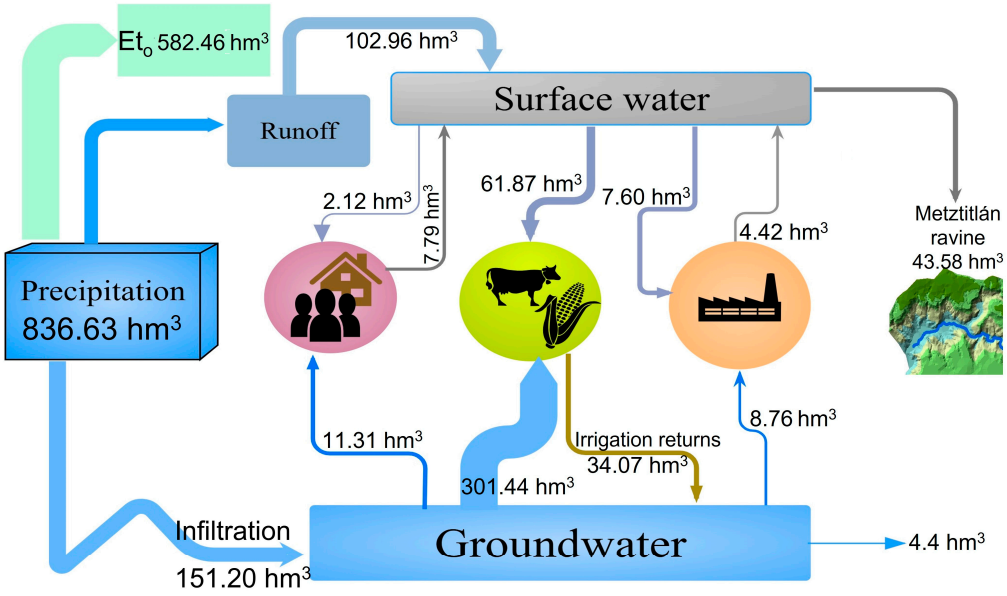

Figure 7. Sankey Flux diagrams of hydrological balance in the Tulancingo Valley. Baseline year 2013.

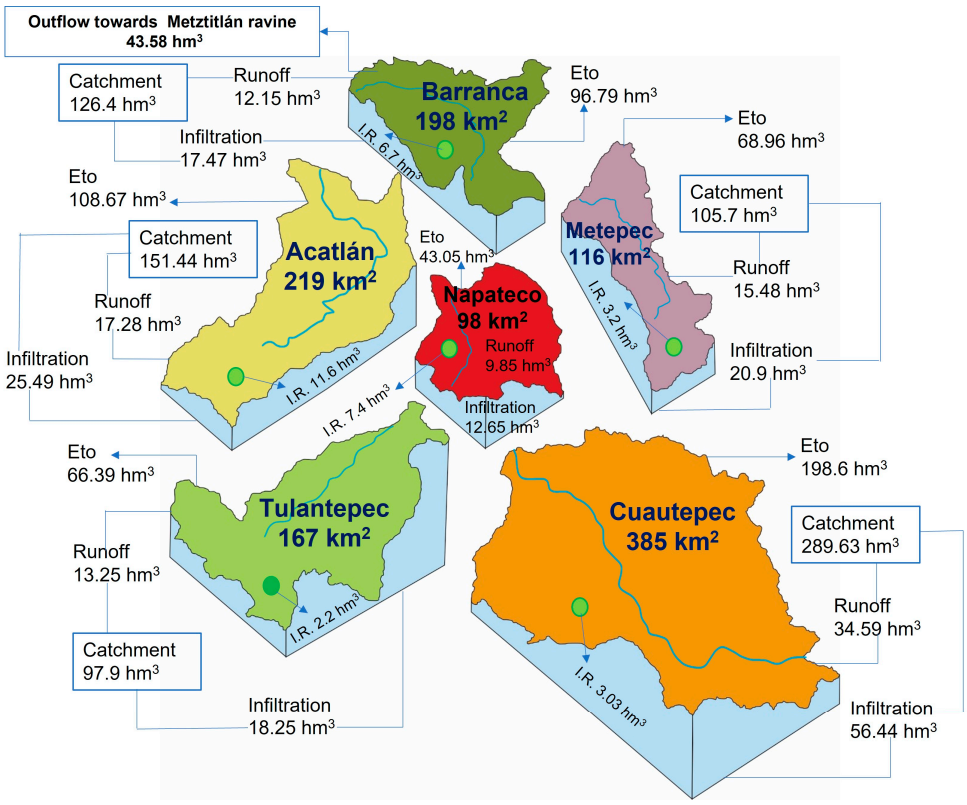

Figure 8. Sub-basins' hydrologic parameters result from the Tulancingo Valley. Baseline year 2013. Eto: evapotranspiration. I.R: irrigation returns.

3.4.1. Sankey Representation of Hydric Metabolism and Balance

Figure 7 shows a Sankey representation of the hydrological components and fluxes interactions in the Tulancingo Valley for the baseline year 2013. The unique input is rainfall, because the principal rivers originate in the valley from runoff of the southern mountains.

Evapotranspiration is highlighted as the model's principal outflow, accounting for 74% of total precipitation entering the valley, as reported in other studies of predominantly agricultural land, such as the warmer Mezquital Valley in Hidalgo State, where 79.2% of precipitation is attributed to evapotranspiration [50]. Those high percentages indicate that areas with use (65.26% in the Tulancingo Valley) also produce elevated evapotranspiration.

3.4.2. Aquifer Balance in the Baseline Year 2013

Aquifer recharge occurs primarily from mountain infiltration surrounding the Tulancingo Valley, irrigation returns, and through geological faults (sinkholes) located mainly in the Cuautepec and Acatlán sub-basins.

The aquifer balance was determined following Equation (2) with average annual total recharge (185.27 hm^3/year), comprising natural discharge (49.4 hm^3/year) and groundwater extraction volume (301.44 + 8.76 + 11.31 hm^3/year). It accounts for an overexploitation of −185.64 hm^3. Lesser et al. [30] reported a deficit in the aquifer as early as the baseline year (−20.9 hm^3).

Surface water in the region is managed with consideration for reserving it for the irrigation district located downstream at the end of the Meztitlán ravine. Consequently, farmers in Tulancingo have no alternative but to rely on groundwater for irrigation. To manage this resource, a private institution was established with local government support to facilitate agreements among farmers and oversee the allocation of concessions. Then, these policies have contributed to groundwater overexploitation. Hence, the measures such as those outlined in M1 and M2 could still be incorporated into management programs.

3.4.3. Sub-Basin Analysis for the Baseline Year 2013

Figure 8 represents the schemes of the six sub-basins that compose the Tulancingo Valley. The components of the hydrological cycle and the territorial extent of each sub-basin are also detailed.

The Cuautepec sub-basin stands out for the highest parameter values because it has the largest surface area, 385 km^2. Runoff is less than infiltration in all sub-basins, since 65.26% of the land surface is plain and devoted to agricultural use, and 25.15% to forest, which promotes higher infiltration within the valley. In comparison, only 2.72% is urban (Figure 1).

3.4.4. Falkenmark Water Stress Index

The average groundwater availability in the Tulancingo Valley was 1050 m^3 per capita per year, indicating water stress according to the threshold established by the authors of [41], calculated using Equation (3) with 151.2 hm^3 of rainfall infiltration distributed among the valley's 242,014 inhabitants.

Because differences exist among sub-basins, we perform individual stress calculations for each one. The Tulantepec sub-basin exhibits absolute scarcity, with only 339 m^3 per capita per year, due to its high population (556 inhabitants/km^2) and the lowest precipitation levels in the valley (97.9 hm^3/year). The Acatlán, Cuautepec, and Napateco sub-basins experience mild water stress, with an estimated per capita availability of 1200 m^3 per year. In contrast, the Barranca and Metepec sub-basins do not exhibit water stress, as they exceed 2500 m^3 per capita per year because of their low population and extensive forested areas.

3.5. Transient Scenarios Results

Table 9 presents the inflow and outflow volumes projected for 2030 and 2050 across all transitional scenarios for the Tulancingo Valley. Table 10 shows the resulting supplied volumes for each sub-basin under all scenarios. For visual comparison, the Sankey diagrams corresponding to the relevant mitigation actions for 2050 are provided in Figures 9 and 10A–C. A detailed analysis is presented in the following sections.

Table 9. Calculated inflow and outflow volumes for 2030 and 2050 in the transition scenarios of the Tulancingo Valley (hm^3/year).

Scenario	Source	2030		2050	
		In-Flow	**Out-Flow**	**In-Flow**	**Out-Flow**
Reference	S.W.	92.12	20.92	56.13	6.03
	G.W.	174.76	−254.34	123.68	−356.94
M1	S.W.	92.12	24.92	56.13	9.03
	G.W.	170.34	−206.34	111.07	−220.94
M2	S.W.	92.12	25.92	56.13	10.03
	G.W.	168.1	−183.34	106.63	−173.94
M3	S.W.	92.12	26.92	56.13	11.03
	G.W.	168.1	−146.34	106.76	−176.94
M4	S.W.	98.61	21.12	62.89	6.33
	G.W.	135.6	−251.64	82.72	−352.14
M5	S.W.	98.11	22.12	63.88	10.63
	G.W.	135.26	−252.64	82.36	−353.14

M1: Irrigation conveyance efficiency improvement, M2: Sprinkler irrigation, M3: Groundwater use substitution by surface water, M4: Physical efficiency, M5: Treatment plant for wastewater reuse.

Table 10. Results of transient scenarios. Surface and groundwater demand in the Tulancingo Valley (hm^3/year).

		2013		2030						2050						
Sub-Basin	**D**	**BL**	**BAU**	**R**	**M1**	**M2**	**M3**	**M4**	**M5**	**BAU**	**R**	**M1**	**M2**	**M3**	**M4**	**M5**
Napateco	G.W.	78	89	91	80	75	87	91	91	97	101	71	61	98	101	100
	S.W.	9	10	10	10	10	14	10	10	10	7	7	7	10	7	7
Metepec	G.W.	27	33	34	30	28	33	34	34	37	42	28	22	35	42	42
	S.W.	9	10	9	8	8	10	9	9	11	6	6	6	13	6	6
Tulantepec	G.W.	23	25	26	24	22	25	25	26	26	30	22	20	26	28	29
	S.W.	8	10	9	8	8	9	9	9	11	7	7	6	12	7	7
Barranca	G.W.	65	93	95	83	77	91	94	95	104	110	75	63	104	109	110
	S.W.	11	11	9	9	9	13	9	9	11	4	4	4	9	4	4
Acatlán	G.W.	119	133	135	117	109	128	135	135	136	145	98	82	135	144	145
	S.W.	14	16	14	14	14	22	14	14	18	9	10	10	20	9	9
Cuautepec	G.W.	9	6	9	8	7	9	8	9	8	12	9	9	12	11	12
	S.W.	20	27	18	15	15	18	18	18	30	14	11	10	14	14	14
Valley	G.W.	322	380	389	342	318	373	387	389	408	440	303	257	410	435	438
	S.W.	72	84	69	64	64	86	69	69	91	48	46	44	79	48	47

D: Demand, G.W: Groundwater demand, S.W: Surface water demand, BL: Base line, BAU: Business-As-Usual, R: Reference (CC: BAU+ Climate change), M1: Irrigation conveyance efficiency improvement, M2: Springler irrigation, M3: Groundwater use substitution by surface water, M4: Physical efficiency, M5: Treatment plant for wastewater reuse.

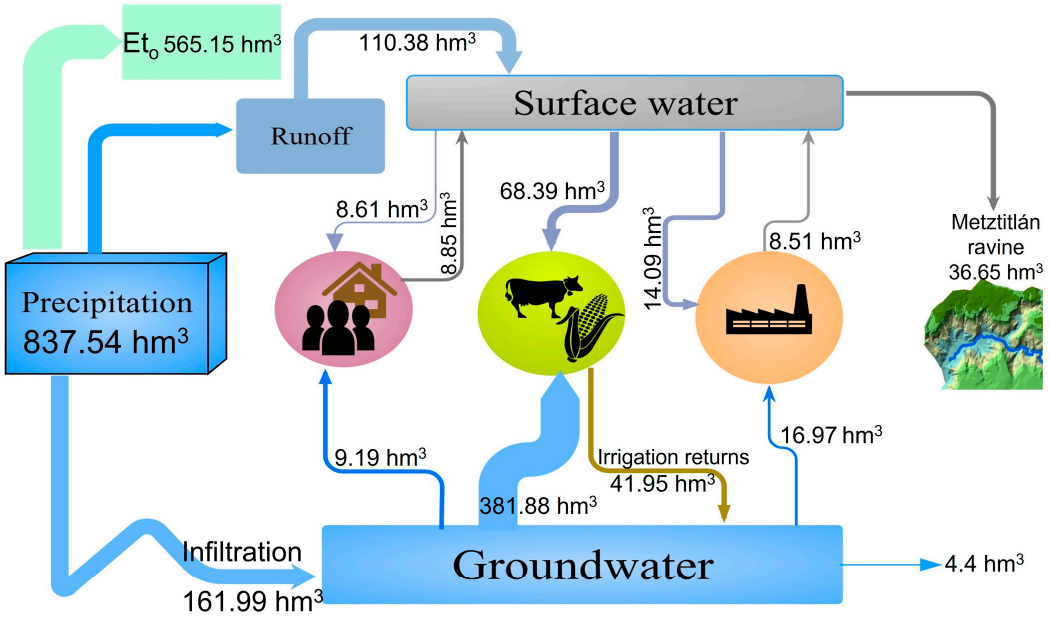

Figure 9. Sankey Flux diagrams of hydrological metabolism in the Tulancingo Valley. Inertial Growth Scenario (BAU) in 2050.

The negative groundwater outflow values reflect the worsening overexploitation of the Tulancingo aquifer, already documented in the baseline year (2013) and primarily driven by agricultural and livestock activities. This pressure on the aquifer can be relieved through the mitigating actions incorporated in scenarios M1–M5.

The inflow and outflow data for all scenarios are shown in Table 9 and are fundamental to any water balance.

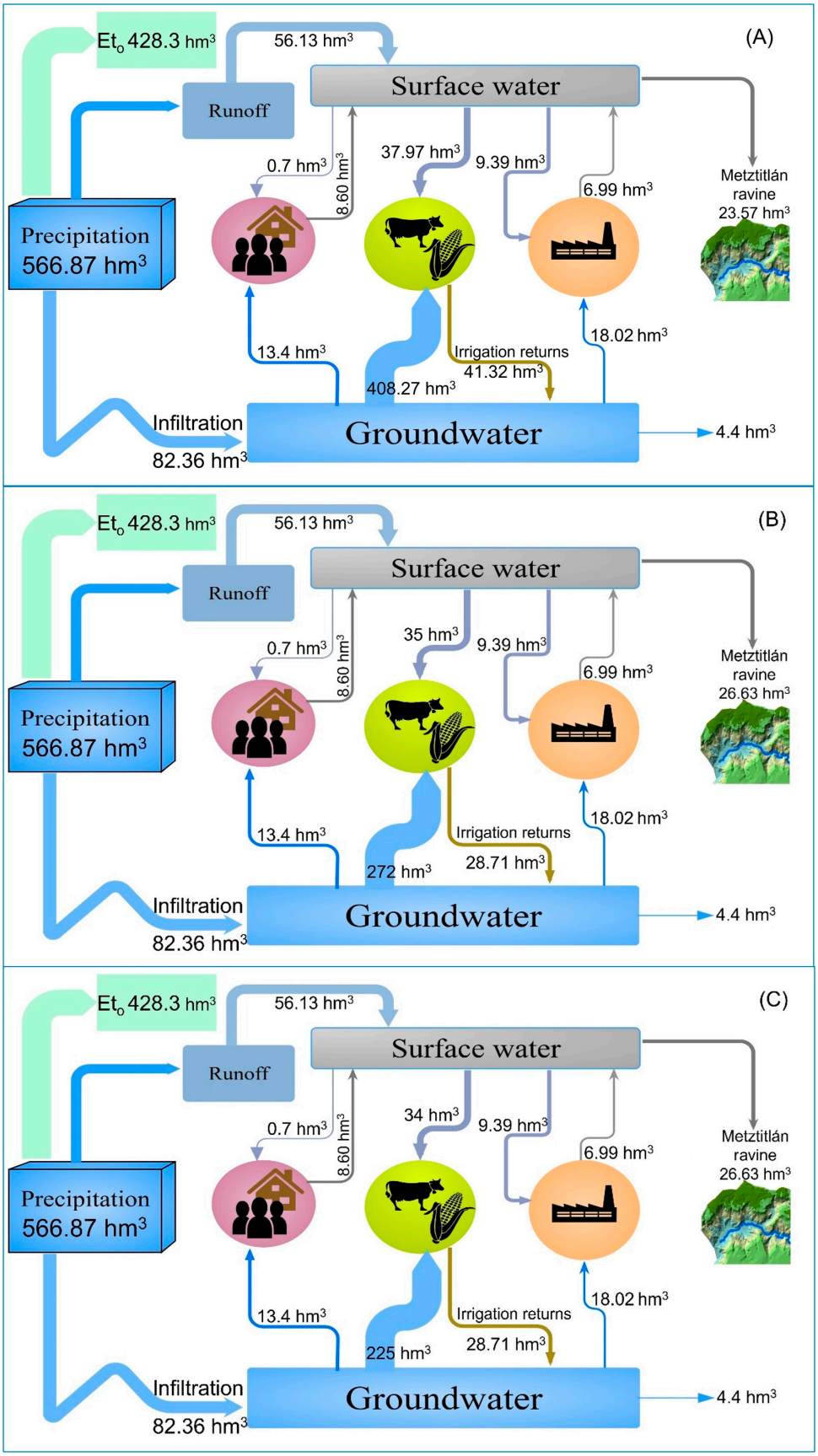

Figure 10. Sankey Flux diagrams of hydrological metabolism in the Tulancingo Valley. (**A**) The Reference scenario (CC), (**B**) irrigation conveyance efficiency improvement, and (**C**) sprinkler irrigation. Year 2050.

3.5.1. Inertial Growth Scenario (BAU)

The estimated surface and groundwater demand volumes for all sectors increases progressively from 2030 onward, consistent with the findings of the authors of [51], who modeled future water demand using WEAP and identified a similar upward trend. The Sankey diagram in Figure 9 illustrates the valley's water balance and the groundwater and surface water demand in 2050 for the BAU scenario.

3.5.2. Climate Change Perturbation Scenario (CC, Reference)

Under the SSP3-RCP7.0 scenario, precipitation is projected to continue declining by −1.5, and temperatures are projected to rise by 1.4 °C to 2050, with significant changes in the valley. The Sankey diagram in Figure 10A illustrates the valley's water balance in 2050, showing rainfall decreases of −269.76 hm^3 and evapotranspiration decreases of −154.09 hm^3 relative to the BAU scenario, despite rising temperatures, reflecting the anticipated reduction in precipitation.

When comparing inertial growth (BAU) with climate-change-induced perturbations, both scenarios exhibit similar patterns in anthropogenic demand for surface and groundwater resources. However, surface water availability declines across all sub-basins, accompanied by reduced aquifer recharge (Table 10), thereby intensifying resource scarcity throughout the valley. Predictably, runoff and infiltration decline, with estimated reductions of 46.83 hm^3 and 68.84 hm^3, respectively, and long-term unmet water demand affecting multiple regions under climate change [17,37,52] reported reductions of 19% in the medium-future scenario and 15% in long-term scenarios. Similar studies report comparable impacts from streamflow reductions under SSP3-RCP4.5 and SSP3-RCP8.5 climate projections, which perturb the hydrological cycle and threaten crop production [17].

Consequently, a recharge deficit for the Tulancingo aquifer amounts to −20.04%, posing a regional water and food security risk by 2050, and the aquifer would reach a demand of −365.12 hm^3 (Figure 10A). These observed effects are consistent with findings from other regions, such as the Mezquital Valley, where projections show a 10% reduction in runoff and infiltration by 2050, facing the same increased demand as the BAU scenario [50]. The Acatlán sub-basin, which accounts for 30.5% of the valley's total agricultural production, would experience the worst outcome.

3.5.3. Agricultural, Urban, and Industrial Mitigation Scenarios

Five mitigation scenarios were calculated to improve water-use efficiency, with emphasis on the agriculture sector, focusing on surface water savings in the Cuautepec sub-basin and protecting aquifer pumping in all. Table 10 shows the effects of the interventions studied for each sub-basin and sector. All actions would improve sustainable management in the valley and prevent aquifer overexploitation, but they would require funding for infrastructure changes.

The mitigation scenarios reveal significant reductions in pressure on the Tulancingo aquifer compared with the Reference scenario across the three sectors, with potential decreases in groundwater extraction by −52.7% and surface water use by −17.2% by 2050 (see Table 10).

Agricultural Sector (M1–M3)

Irrigation conveyance efficiency improvement (M1). This action would produce an estimated 33.3% reduction in groundwater extraction and a 7.9% reduction in surface water use in the Tulancingo Valley by 2050. The Cuautepec sub-basin would stand out for a 30% reduction in surface water use, as it hosts the leading agricultural irrigation canal network, distributing water to the southern valley. Gradual canal lining yields a significant increase

in efficiency and better resource use. Prior studies reported similar results, with a 17% reduction in total water use over the simulation period using WEAP modeling [13]. This action would significantly reduce aquifer pumping volumes in 2050, achieving 136.3 hm^3. Table 11 shows the mitigation potential, and Figure 10B shows the Sankey diagram for 2050.

Table 11. Cumulative effects on the Tulancingo aquifer due to disturbances in 2030 and 2050 (hm^3).

	Action	Disturbance	2030	2050	Net Effect in 2050
Inertial Demand	Agriculture Population Industry	Pumping increases	−64.26 −0.19 −3.28	−106.8 −2.11 −9.26	−187.04
	Climate change	Decreases infiltration *	−15.94	−68.84	
Agriculture Mitigation	Irrigation canals (M1) Sparkling irrigation (M2) Surface water subst. (M3)	Pumping decreases	47.7 70.7 18.2	136.3 182.8 31.8	225.4
Urban Mitigation	Physical efficiency (M4)		2.7	4.5	4.5
Industrial Mitigation	Wastewater plant (M5)		0.0	1.8	1.8
Total mitigation potential calculated from 2026 to 2050					231.7

* Difference between Scenario CC and BAU.

Sprinkler irrigation (M2). This action would mitigate total groundwater demand in the valley by 44.9% and surface water demand by 10.5%. In agriculturally dominant areas, sprinkler systems would reduce groundwater use by 44.7% in the Acatlán sub-basin by 2050, representing a potential saving of 63 hm^3. In addition, sprinkler systems increase crop yields, underscoring their dual benefit for labor costs. Productivity as crop water stress is reduced [53–55]. As in M1, this action would significantly reduce aquifer pumping volume to 182.8 hm^3 in 2050. Table 11 shows the mitigation potential, and Figure 10C shows the Sankey diagram for 2050.

Substituting groundwater with surface water (M3): This is projected to reduce groundwater use by 30 hm^3 annually (a 7.4% decrease) and increase valley-wide surface water demand by 81.6% by 2050. Although the Acatlán sub-basin shows the most extensive groundwater use, its reduction potential is low (7.1%) because the available flow rate is approximately 8.4 hm^3. This limits the percentage of groundwater that can be replaced by surface water. It is estimated that, by 2050, this sub-basin will require 141 hm^3 to support its agricultural activities, taking into account the impacts of climate change and the gradual growth of the sector. The Cuautepec sub-basin already has rainfed agriculture and an irrigation network of canals for surface water. Hence, the actions were simulated in the other four sub-basins. In 2050, the mitigation potential is the lowest in this sector, 31.8 hm^3.

Urban Sector

Physical efficiency (M4). Increasing distribution system efficiency to 75% through leak repairs reduces groundwater demand by 35.8% and surface water demand by 42.9%. Although these percentages are substantial, the absolute volumes remain low because the valley's population is relatively small. Gradual leak repair in urban distribution networks significantly decreases demand over time [40]. Effective management of urban water production and distribution subprocesses is essential for achieving resource-use efficiency [56]. The mitigation potential in this sector in 2050 is comparatively small—4.5 hm^3—due to the low population of the Tulancingo Valley (See Table 11). Unlike Rios et al., who found urban efficiency most impactful in the Cuautitlán–Pachuca Valley [41],

our results evidence that agriculture dominates in the region. This reflects the valley's agrarian context versus an urban basin.

Industrial Sector

The textile industry is the largest industrial water consumer in the valley; therefore, installing a treatment plant in each sub-basin was proposed to enable the recycling and reuse of industrial wastewater in subsequent textile dyeing processes [57], while also reducing the considerable environmental impacts associated with this sector [58]. This measure would reduce total surface water demand by 40.4% and groundwater demand by 21.2%. Previous studies indicate that treating 50 m^3/day of textile wastewater from the bleaching process can be achieved with a treatment plant equipped with sweep gas membrane technology. Sangare et al. report that implementing wastewater reuse systems can reduce river pollution by up to 86% [12]. Industries adopting this measure could, therefore, reuse treated water for irrigating green areas, thereby enhancing infiltration and contributing to the recharge of the Tulancingo aquifer. Despite this sector having the highest economic value, it presents the lowest mitigation potential of −1.8 hm^3 in 2050.

3.6. Cumulative Effects on Groundwater in the Tulancingo Valley

Given the importance and threat to the aquifer, we show the timeline evolution of agricultural (Figure 11A), urban (Figure 11B), and industrial (Figure 11C) groundwater use for each proposed mitigation action.

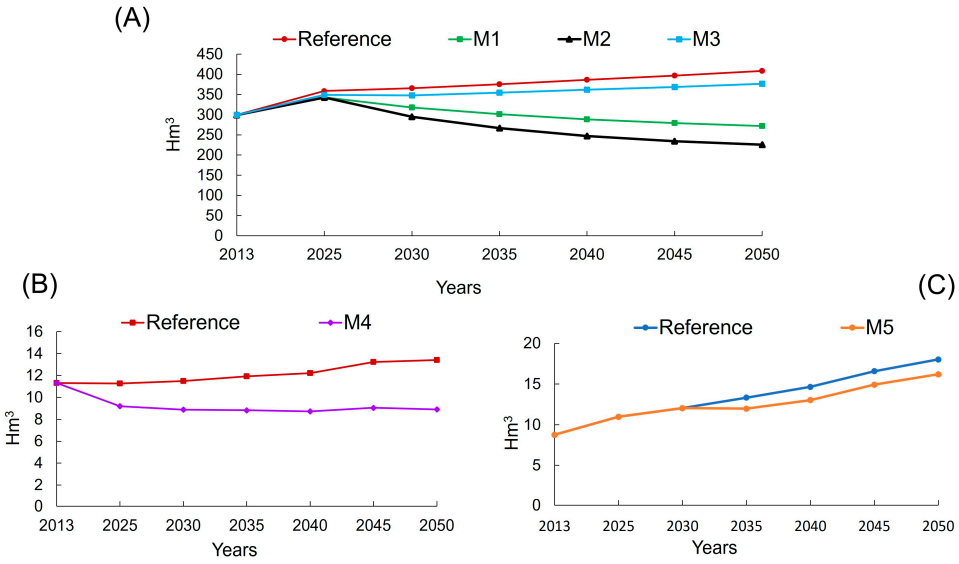

Figure 11. Groundwater demands mitigation scenarios. (**A**) Agricultural sector, (**B**) urban sector, and (**C**) industrial sector.

A marked decrease in groundwater demand is observed from 2025 onward relative to the Reference scenario, driven largely by reductions in the agricultural sector (Figure 11A). The analysis also shows that, if mitigation measures are applied only to the urban and industrial sectors, demand reduction would be minimal, since the valley's most significant water demand originates from agricultural activities.

By the end of the simulation period, the combined effect of all three sectors and all mitigation measures could reduce total groundwater demand in the valley by 52.7%, indicating that the proposed actions are viable for improving water management.

3.7. Cumulative Effects on Aquifer Volumes

Previous analyses have shown that agricultural water demand represents the greatest threat to the region's water resources, particularly the aquifer. When the cumulative effects on aquifer volumes are evaluated under the assumptions of no mitigation measures, continued growth in demand across the three sectors, and reduced infiltration due to climate change, the valley is projected to experience a net deficit of −187.04 hm^3 by 2050, as detailed in Table 11.

In contrast, the combined mitigation potential (positive values) of the proposed measures across all three sectors amounts to 231.7 hm^3 by 2050. Theoretically, if these measures are effectively implemented, they could substantially reverse the deficit and significantly reduce the aquifer overexploitation that has persisted since 2013 [32]. These mitigation potentials are calculated as the difference between the volumes calculated in each mitigation scenario and the corresponding volumes in the reference (CC) scenario.

Table 11 illustrates the potential for restoring the aquifer's balance under sustained intervention and provides a basis for conducting a cost–benefit assessment to establish an appropriate hierarchy of actions. This process will define suitable policy programs and final decisions.

By 2030, cumulative savings are modest but measurable, especially in sub-basins with early substitution (e.g., Metepec, Tulantepec, and Napateco). By 2050, savings increase significantly due to the full implementation of mitigation strategies and time cumulative effects.

3.8. Limitations and Future Perspectives

3.8.1. Limitations

Data limitations. The modeling relied on the official datasets available at the time, and industrial water-supply information from REPDA was limited for the base year. As a result, actual industrial water demand is likely higher than the calculated values. However, this limitation has a negligible effect on the overall water supply assessment, as the industrial sector accounts for only a small share of total demand in the valley.

Tulancingo Valley is covered by a network of 15 meteorological stations, which allows for more precise precipitation and temperature projections; therefore, this is not a major limitation. In contrast, this study was constrained to establish 2013 as the base year because no more recent hydrometric data were available for model calibration, and this reference point is now relatively distant in time. This limitation is unavoidable, and the absence of post-2013 hydrometric records may undermine confidence in long-term projections, even though relative scenario comparisons remain valid. The results should be interpreted as indicative for decision-makers and allow a preliminary estimation of the cost-benefit ratio.

Complex governance and complementary measures. The study area comprises three major water-use sectors, which create complex water-resource management challenges. The proposed mitigation actions should require additional infrastructure, and the related costs and benefits should be calculated to prioritize the actions to prevent irreversible aquifer deterioration and increase natural recharge.

Priority actions include basin management plans that promote the efficient, rational use of both groundwater and surface water, integrated irrigation management to reduce supply losses, and the conservation of forests and water bodies, all of which are essential to water sustainability. Coordinated governance and stakeholder engagement are viable strategies [41,59,60].

Trends affecting recharge. Increasing surface and groundwater demands are concerning, given agricultural expansion, precipitation variability, a 4.15% reduction in water

bodies, and a 1.42% loss of forest area, all of which are key to natural recharge and surface water harvesting.

3.8.2. Recommended Actions

Wastewater regulation and urban runoff management. Effective regulation of wastewater generation and disposal in industrial and urban sectors is crucial to prevent environmental degradation. Poorly managed discharges and impermeable urban infrastructure reduce infiltration capacity. Long-term sustainable urban runoff measures, such as rain gardens and bioretention systems, have been used in semi-arid zones to mitigate environmental and social impacts [61].

Stakeholder engagement and demand management. The success of any water-saving strategy depends on strengthening awareness and participation among stakeholders [62]. Given that the aquifer is the valley's only reliable freshwater source, stakeholders must adopt a strategic approach to protecting it, as surface water availability is limited. This includes improving canal lining, enhancing irrigation efficiency, and promoting responsible water use across sectors.

Final outlook. Water availability in the Tulancingo Valley is projected to face increasing pressure under future conditions. However, implementing the mitigation measures proposed in this study across the three sectors and complementing them with the additional actions described above can reduce demand, improve efficiency, and support the region's long-term sustainable development.

Overall impact: the modeled mitigation package substantially reduces pressure on the Tulancingo aquifer and surface water abstractions, supporting a transition toward more sustainable water balances under future scenarios.

4. Conclusions

The mathematical model approach, based on sub-basins, is valid and representative of the system. Sectoral analyses enable the integration or tailoring of targeted measures to deliver social, environmental, and economic benefits. Evapotranspiration is the primary model outflow. Infiltration exceeds runoff in all sub-basins because most of the land is used for agriculture or is forested, promoting infiltration across the valley. Groundwater demands in the valley are substantially higher than surface water demands, particularly in the agricultural sector, placing the Tulancingo aquifer in a vulnerable state.

Predictive models estimate that, if demands in the three sectors continue to grow and climate change effects materialize, the valley would face a deficit of 187.04 hm^3 by 2050, threatening groundwater and surface water availability, water security, and regional food security. Implementing the proposed mitigation measures yields a theoretical mitigation potential of 231.7 hm^3 by the end of the simulation period, supporting long-term sustainable water availability in the Tulancingo Valley. Principal actions include gradual increases in sprinkler irrigation efficiency and canal lining to improve water management in agricultural regions. Urban and industrial efficiency measures, such as leak repairs and greywater reuse, are reliable strategies for sustainable water-resource management in the valley through 2050 without compromising future resources.

The results support strategies for efficient water use and integrated management in an agricultural basin, especially with intensifying aquifer overexploitation.

Supplementary Materials: The following supporting information can be downloaded at: https://www.mdpi.com/article/10.3390/hydrology13030077/s1. Figure S1: Average precipitation and temperature values for Tulancingo Valley from 1998 to 2017. Figure S2: Standardized precipitation index from 1998 to 2017 in the Tulancingo Valley; Table S1: Falkenmark Index Ranking; Table S2: Population projections for sub-basins of the Tulancingo Valley. Table S3: Land use and sub-basin percentage used

in the WEAP Interp Function for 2020 and 2030 years. Table S4: Land use and sub-basin percentage used in the WEAP Interp Function for 2040 and 2050 years. Equation (S1): Evapotranspiration by the Penman–Monteith method.

Author Contributions: Conceptualization, E.M.O.-S. and A.D.R.-G.; methodology, software, and validation, G.I.Á.-C. and S.C.-C.; formal analysis, G.M.V.-C.; investigation and data curation, G.I.Á.-C.; writing—original draft preparation, S.C.-C.; A.D.R.-G., G.I.Á.-C. and G.M.V.-C.; final writing—review and editing, E.M.O.-S.; visualization, G.M.V.-C. and E.M.O.-S.; supervision, S.C.-C., A.D.R.-G. and E.M.O.-S. All authors have read and agreed to the published version of the manuscript.

Funding: This research received no external funding. G.I.A-C. received a scholarship from Secretariat of Science, Humanities, Technology, and Innovation, Mexico, for her PhD studies.

Data Availability Statement: The database used in this study is publicly available online. See online data references.

Acknowledgments: The authors thank Hidalgo State Autonomous University for the logistical support. G.I.A.C. is grateful for the doctoral scholarship 289499 from the Secretariat of Science, Humanities, Technology, and Innovation (SECIHTI).

Conflicts of Interest: The authors declare no conflicts of interest. The funders had no role in the study's design, in the collection, analyses, or interpretation of data, in the writing of the manuscript, or in the decision to publish the results.

References

1. Chakraborty, S.K. (Ed.) Water: Its Properties, Distribution, and Significance. In *Riverine Ecology. Eco-Functionality of the Physical Environment of Rivers*; Springer Nature: Cham, Switzerland, 2021; Volume 1, pp. 23–55. [CrossRef]
2. iAgua. ¿Cuánta Agua Subterránea Hay en el Mundo?: Distribución por Continentes y Países. Available online: https://www.iagua.es/respuestas/cuanta-agua-subterranea-hay-mundo-distribucion-continentes-y-paises?utm_source=chatgpt.com (accessed on 7 September 2025).
3. World Bank Group. (W.B.G.). Water for Planet. Available online: https://www.worldbank.org/en/topic/waterresourcesmanagement (accessed on 21 February 2025).
4. Aquae. Causas de la Escasez de Agua en el Mundo. Available online: https://www.fundacionaquae.org/wiki/escasez-de-agua-en-el-mundo-naciones-unidas-advierte-que-la-demanda-crecera-hasta-un-30-por-ciento-en-2050/ (accessed on 12 March 2025).
5. Li, X.; Huang, G.; Wang, S.; Li, Y.; Zhang, X.; Luo, B. Development of an optimization-driven equilibrium model for managing water consumption and its socioeconomic effects. *Sustain. Cities Soc.* **2025**, *118*, 106038. [CrossRef]
6. Vardon, M.; Lien, L.T.H.; Martinez-Lagunes, R.; Batlokwa, P.O.; Schenau, S.; May, S.; Quentin, G.R. Accounting for water: A global review and indicators of best practice for improved water governance. *Ecol. Econ.* **2025**, *227*, 108396. [CrossRef]
7. Guo, T.; Ji, T.; Yan, X.; Yehia Mady, A.; Liu, R.; Huang, M. Temporal variations of soil saturated hydraulic conductivity under different land use types and its impact on water balance components. *Agric. Water Manag.* **2025**, *315*, 109557. [CrossRef]
8. Lima-Quispe, N.; Ruelland, D.; Rabatel, A.; Lavado-Casimiro, W.; Condom, T. Modeling Lake Titicaca's water balance: The dominant roles of precipitation and evaporation. *Hydrol. Earth Syst. Sci.* **2025**, *29*, 655–682. [CrossRef]
9. Kalashnikova, O.; Niyazov, J.; Nurbatsina, A. Hydrological Modeling in Studies of Mountain River Basins of Central Asia. *Georgian Geogr. J.* **2024**, *4*, 38–47. [CrossRef]
10. Ahmad, S.; Waseem, M.; Wahab, H.; Khan, A.Q.; Jehan, Z.; Ahmad, I.; Leta, M.K. Assessing water demand and supply in the Upper Indus Basin using integrated hydrological modeling under varied socioeconomic scenarios. *Appl. Water Sci.* **2024**, *15*, 5. [CrossRef]
11. Mahmoodzadeh, D.; Morid, S.; Ketabchi, H. Assessment of water resources sustainability under unilateral development projects using the WEAP model in transboundary river basins. *Environ. Sci. Pollut. Res.* **2025**, *32*, 6130–6152. [CrossRef] [PubMed]
12. Sangaré, L.O.; Ba, S.; Hu, N.; Coulibaly, D.; Konté, M.S.; Ly, O.; Zheng, T. Hydrological simulation scenarios for predicting the future water status of the Niger River in Bamako, Mali, for sustainable development. *Environ. Sci. Pollut. Res.* **2025**, *32*, 4957–4974. [CrossRef]
13. Sibale, D.; Kranjac-Berisavljevic, G.; Abdul-Ganiyu, S. Evaluation of water delivery performance of the Bontanga irrigation scheme in the Northern Region of Ghana. *Water Pract. Technol.* **2025**, *20*, 298–313. [CrossRef]
14. Khan, H.; Bin Zaid, Z. Projecting irrigation demand under IPCC climate change scenarios using WEAP modeling in the Rechna Doab, Pakistan. *Clean. Water* **2024**, *2*, 100040. [CrossRef]

15. Ansari, A.; Pranesti, A.; Telaumbanua, M.; Alam, T.; Wulandari, R.A.; Nugroho, B.D.A. Evaluating the effect of climate change on rice production in Indonesia using a multimodal approach. *Heliyon* **2023**, *9*, e19639. [CrossRef]
16. Calizaya-Tercero, A.; Mendoza, J.; Copa, M. Hydrological bases for the natural resources conservation in the Lake Moa catchment, Bolivia. *Reg. Water Conserv.* **2025**, *8*, 78–93. [CrossRef]
17. Hirko, D.B.; Du Plessis, J.A.; Bosman, A. Review of machine learning and WEAP models for water allocation under climate change. *Earth Sci. Inform.* **2025**, *18*, 310. [CrossRef]
18. Wang, Y.; Xie, Y.; Qi, L.; He, Y.; Bo, H. Synergies evaluation and influencing factors analysis of the water–energy–food nexus from symbiosis perspective: A case study in the Beijing–Tianjin–Hebei region. *Sci. Total Environ.* **2022**, *818*, 151731. [CrossRef] [PubMed]
19. Ahmad, R.; Liu, G.; Ur Rehman, S.A.; Gao, Y.; Meng, F.; Zhou, X.; Liu, B.; Cristiano, S. Integrated Systems Modeling for Assessing the Water–Energy Nexus in Pakistan: Lessons Learned From Coupling LEAP–WEAP Planning Approaches. *Engineering* **2025**, *50*, 72–87. [CrossRef]
20. Arcega, I.; Otazo, E.; Galindo, E.; Acevedo, O.; Romo, C. Determinación del índice de vulnerabilidad mediante el método DRASTIC Caso: Acuífero del Valle de Tulancingo, Hidalgo, México. *Rev. Iberoam. Cienc.* **2015**, *2*, 39–49.
21. SIATL. Available online: https://antares.inegi.org.mx/analisis/red_hidro/siatl/# (accessed on 19 October 2023).
22. DENUE. Directorio Estadístico Nacional de Unidades Económicas. Available online: https://www.inegi.org.mx/app/mapa/denue/default.aspx (accessed on 28 July 2024).
23. INEGI. Censo de Población y Vivienda (CPV) 2020. Available online: https://www.inegi.org.mx/programas/ccpv/2020/ (accessed on 7 October 2023).
24. INEGI. Guía para la Interpretación de Cartografía. Edafología. Available online: https://www.inegi.org.mx/app/biblioteca/ficha.html?upc=702825231736 (accessed on 27 November 2023).
25. SMN. Información Estadística Climatológica. Available online: https://smn.conagua.gob.mx/es/climatologia/informacion-climatologica/informacion-estadistica-climatologica (accessed on 2 May 2023).
26. Ortiz, E.; Villaseñor, J.L. Una propuesta de actualización del mapa de vegetación potencial de México. *Bot. Sci.* **2025**, *103*, 381–393. [CrossRef]
27. CONAGUA. Available online: https://app.conagua.gob.mx/consultarepda.aspx (accessed on 12 January 2024).
28. Torres Suárez, S.L.; Tijerina Chávez, L.; Ibáñez Castillo, L.A.; Bautista Hernández, M. Optimización de recursos en la producción de forrajes del distrito de riego 028 de Tulancingo. *Rev. Mex. Cienc. Agrícolas* **2020**, *24*, 153–163. Available online: https://cienciasagricolas.inifap.gob.mx/index.php/agricolas/article/view/2366/3077 (accessed on 26 March 2024).
29. SIGACUA. Available online: https://sigagis.conagua.gob.mx/gas1/sections/Edos/hidalgo/hidalgo.html (accessed on 26 March 2024).
30. Lesser, I.J.M.; Arellano, I.S.; González, P.D.; Lesser, C.L.E. Balance y Modelo del Acuífero de Tulancingo, Hidalgo. Executive Report. 2006. Available online: https://www.lesser.mx/files/07-1-Tulancingo.pdf (accessed on 12 January 2024).
31. Fernández, V. Iniciarán la Limpieza de Resumideros de Tulancingo. Available online: https://oem.com.mx/elsoldetulancingo/local/iniciaran-la-limpieza-de-resumideros-de-tulancingo-19118411 (accessed on 15 June 2024).
32. CONAGUA. Available online: https://www.dof.gob.mx/nota_detalle.php?codigo=5320583&fecha=04/11/2013#gsc.tab=0 (accessed on 19 July 2023).
33. SIAP. Available online: https://nube.siap.gob.mx/cierreagricola/ (accessed on 9 December 2023).
34. Guerrero Rodríguez, W.J.; Gómez Aldapa, C.A.; González Ramírez, C.A.; Castro Rosas, J. Lactosuero y su problemática en el medio ambiente. In *Proceedings of the XI National Congress of Food Science and Technology*; Universidad Autónoma de Nuevo León: Monterrey, Mexico, 2017. Available online: https://silo.tips/download/xi-congreso-nacional-de-ciencia-y-tecnologia-de-alimentos-lunes-31-de-agosto-y-e (accessed on 25 November 2024).
35. Sieber, J.P. Available online: http://www.weap21.org/downloads/WEAP_User_Guide.pdf (accessed on 18 January 2024).
36. INEGI. Continuo de Elevaciones Mexicano y Modelos Digitales de Elevación. Available online: https://www.inegi.org.mx/app/geo2/elevacionesmex/ (accessed on 22 November 2023).
37. Dlamini, N.; Senzanje, A.; Mabhaudhi, T. Assessing climate change impacts on surface water availability using the WEAP model: A case study of the Buffalo River catchment, South Africa. *J. Hydrol. Reg. Stud.* **2023**, *46*, 101330. [CrossRef]
38. Zotarelli, L.; Dukes, M.D.; Romero, C.C.; Migliaccio, K.W.; Morgan, K.T. Step by Step Calculation of the Penman-Monteith Evapotranspiration (FAO-56 Method). Available online: http://edis.ifas.ufl.edu/pdffiles/ae/ae45900.pdf (accessed on 22 November 2023).
39. Galindo, E.; Otazo, E.M.; Reyes, L.R.; Arellano, S.M.; Gordillo, A.; González, C.A. Balance hídrico y afectaciones a la recarga del acuífero Cuautitlán-Pachuca para el año 2021. *GeoFocus Int. Rev. Geogr. Inf. Sci. Technol.* **2010**, *10*, 65–90. Available online: https://www.geofocus.org/index.php/geofocus/article/view/206 (accessed on 22 November 2023).
40. Gómez, A.A. Rentabilidad e Impacto Ambiental de la Quesería en el Valle de Tulancingo, Hidalgo. Ph.D. Thesis, Universidad Autónoma Chapingo, Texcoco, Mexico, 2010.

41. Ríos-Sánchez, K.I.; Chamizo-Checa, S.; Galindo-Castillo, E.; Acevedo-Sandoval, O.A.; González-Ramírez, C.A.; Hernández-Flores, M.D.; Otazo-Sánchez, E.M. The Groundwater Management in the Mexico Megacity Peri-Urban Interface. *Sustainability* **2024**, *16*, 4801. [CrossRef]
42. Allen, R.G.; Pereira, L.S.; Raes, D.; Smith, M. *Crop Evapotranspiration: Guidelines for Computing Crop Water Requirements*; FAO Irrigation and Drainage Paper. No. 56; Food and Agriculture Organization of the United Nations: Rome, Italy, 1998. Available online: https://www.fao.org/4/x0490s/x0490s00.htm (accessed on 8 February 2026).
43. Falkenmark, M. The Massive Water Scarcity Now Threatening Africa: Why Isn't It Being Addressed? *Ambio* **1989**, *18*, 112–118.
44. Consejo Estatal de Población. Available online: https://poblacion.hidalgo.gob.mx/Proyec (accessed on 17 March 2024).
45. INEGI. Available online: http://geoportal.conabio.gob.mx/metadatos/doc/html/usv250s5ugw.html (accessed on 12 August 2023).
46. INEGI. Available online: http://www.conabio.gob.mx/informacion/gis/?vns=gis_root/usv/inegi/usv250s5ugw (accessed on 12 August 2023).
47. IPCC. IPCC WGI Interactive Atlas. Available online: https://interactive-atlas.ipcc.ch/regional (accessed on 7 November 2023).
48. CONAGUA. Manuales de Operación y Especificaciones Técnicas del Programa de Apoyo a la Infraestructura Hidroagrícola S217. Available online: https://www.gob.mx/conagua/documentos/manuales-de-operacion-y-especificaciones-tecnicas (accessed on 16 September 2025).
49. Azanaw, A.; Birlie, B.; Teshome, B.; Jemberie, M. Textile effluent treatment methods and eco-friendly resolution of textile wastewater. *Case Stud. Chem. Environ. Eng.* **2022**, *6*, 100230. [CrossRef]
50. Chamizo-Checa, S.; Otazo-Sánchez, E.; Gordillo-Martínez, A.; Suárez-Sánchez, J.; González-Ramírez, C.; Muñoz-Nava, H. Megacity Wastewater Poured into a Nearby Basin: Looking for Sustainable Scenarios in a Case Study. *Water* **2020**, *12*, 824. [CrossRef]
51. Dias, I.Y.; Lazaro, L.L.; Barros, V.G. Water–Energy–Food Security Nexus—Estimating Future Water Demand Scenarios Based on Nexus Thinking: The Watershed as a Territory. *Sustainability* **2023**, *15*, 7050. [CrossRef]
52. Dau, Q.V.; Adeloye, A.J. Water security implications of climate and socio-economic stressors for river basin management. *Hydrol. Sci. J.* **2021**, *66*, 1097–1112. [CrossRef]
53. Araya-Portuguez, K.; Fuentes-Quirós, G.F.-Q. Sistema de riego automatizado para zonas rurales. *Rev. Tecnol. Marcha* **2024**, *37*, 92–102. [CrossRef]
54. Morchid, A.; Et-taibi, B.; Oughannou, Z.; El Alami, R.; Qjidaa, H.; Jamil, M.O.; Boufounas, E.M.; Abid, M.R. IoT-enabled smart agriculture for improving water management: A smart irrigation control using embedded systems and Server-Sent Events. *Sci. Afr.* **2025**, *27*, e02527. [CrossRef]
55. Sharifi, S.; Asakereh, A.; Kiani Deh Kiani, M.; Janatrostami, S. Investigation, modeling, and optimization nexus of water, energy, and food in paddy production in Rasht County. *Iran. J. Biosyst. Eng.* **2025**, *55*, 21–43. [CrossRef]
56. Yin, C.; Hsiao, B.; See, K.F. Efficiency analysis of China's urban water supply utilities using a dynamic multiactivity network DEA model. *Struct. Change Econ. Dyn.* **2024**, *71*, 387–404. [CrossRef]
57. Orts, F.; del Río, A.I.; Molina, J.; Bonastre, J.; Cases, F. Study of the Reuse of Industrial Wastewater After Electrochemical Treatment of Textile Effluents without External Addition of Chloride. *Int. J. Electrochem. Sci.* **2019**, *14*, 1733–1750. [CrossRef]
58. Monmeneu, V.G. Diseño de un Sistema que Integra Destilación por Membranas para el Tratamiento de 50 m^3/día de Aguas Residuales Textiles del Proceso de Blanqueo; Tesis de Grado en Ingeniería Química; Universitat Politècnica de València: València, Spain, 2025. Available online: https://riunet.upv.es/handle/10251/226935 (accessed on 16 September 2025).
59. Bassi, N.; Chaturvedi, V. Balance hídrico y enfoque de distribución de beneficios para reducir el déficit hídrico en una cuenca fluvial de la India. *Rev. Int. Desarro. Recur. Hídr.* **2024**, *40*, 604–626. [CrossRef]
60. Abd Rani, M.N.; Md Khalid, R. Legal frameworks and mechanisms for resolving transboundary water disputes in Malaysia: Insights from the Kedah-Penang Muda River dispute. *Int. J. Water Resour. Dev.* **2025**, *41*, 625–646. [CrossRef]
61. Majid, D.; Al Kholif, M.; Arif, M.N.; Sutrisno, J.; Zhang, J.W. Eco-friendly solutions for urban wastewater: Evaluating constructed wetlands and filtration methods. *Adv. Environ. Technol.* **2025**, *11*, 182–194. [CrossRef]
62. Zheng, H.; Wang, H.; He, H.; Wu, Y.; Delang, C.O.; Wu, J.; Lu, J.; Yao, Z.; Hu, Y.; Gomez, C. Quantifying the heterogeneity in urban water resource utilization efficiency using a meta-frontier super SBM model: Application in the Yellow River Basin. *J. Clean. Prod.* **2024**, *485*, 144410. [CrossRef]

Disclaimer/Publisher's Note: The statements, opinions and data contained in all publications are solely those of the individual author(s) and contributor(s) and not of MDPI and/or the editor(s). MDPI and/or the editor(s) disclaim responsibility for any injury to people or property resulting from any ideas, methods, instructions or products referred to in the content.